Effects of Variable Viscosity and Thermal Conductivity on MHD Free Convective Flow Along a Vertical Porous Plate with Viscous Dissipation

G.C. Hazarika[#1], Jadav Konch[*2]

[#]*Professor and Head Department of Mathematics,*
Dibrugarh University, Dibrugarh-786004, Assam, India
[*]*Department of Mathematics, Dibrugarh University,*
Dibrugarh-786004, Assam, India

***Abstract*— Effects of temperature dependent viscosity and thermal conductivity on a two-dimensional steady laminar MHD free convective flow over a vertical porous flat plate immersed in porous medium with viscous dissipation and heat generation have been studied in the present work. The boundary layer equations are transformed into ordinary differential equations using similarity transformations. The effects of variable viscosity, variable thermal conductivity and the parameters involved in the study on the velocity, temperature and concentration profiles are investigated by solving the governing transformed ordinary differential equations with the help of Runge-Kutta shooting method and shown graphically and in tabulated form and discussed in detail. The effects are significant.**

***Keywords*— Variable viscosity, variable thermal conductivity, viscous dissipation, porous medium, skin-friction, heat transfer, mass transfer.**

I. INTRODUCTION

The study of free convection flows, which occur in nature have become a potential topics because of its wide applicability in geophysical and industrial fields such as chemical engineering process or drying process. By using electrically conducting fluids and the magnetic fields one can control many metallurgical processes involving cooling of continuous strips. The practical importance of heat generation or absorption effects is followed in some physical problems such fluids undergoing exothermic or endothermic chemical reactions. Raptis and Perdikis[1] investigated viscous flow for a non-linearly stretching sheet with chemical reaction and magnetic field. Samad et al. [2] studied natural convection flow through a porous medium considering the effect of magnetic field with thermal radiation, viscous dissipation and variable suction. The influence of magnetic field on heat and mass transfer by natural convection from vertical surfaces in porous media with Soret and Dufour effects has been carried out by Postelnicu [3]. Ahammad and Mollah [4] studied the MHD free convection flow and mass transfer problem over a stretching sheet considering Dufour & Soret effects with magnetic field. In the presence of a magnetic field natural convection for an electrically conducting fluid was analyzed by Lykoudis [5]. Gupta [6] discussed steady and transient free convection of an electrically conducting fluid from a vertical plate in the presence of magnetic field. Ravikumar et al. [7] carried out a steady free convective and mass transfer flow of an electrically conducting viscous fluid through a porous medium bounded by two vertical plates. Dufour and Soret effects on free-forced convection flow past a vertical porous plate immersed in a porous medium for a hydrogen-air mixture as the non-chemical reacting fluid pair was reported by Alam et al. [8]. Further Alam et al. [9] took into account the viscous dissipation effects on MHD natural convection boundary layer flow over a sphere of an electrically conducting fluid in the presence of heat generation. They reported that for increasing values of heat generation parameter, the skin-friction coefficient increases whereas the Nusselt number decreases significantly within the boundary layer. Sattar and Kalim [10] presented unsteady free convection interaction in a boundary layer flow past a vertical porous plate with thermal radiation. Kairi and Murthy [11] investigated the Soret effect with the influence of variable viscosity on natural convection from a melting vertical surface in a non-Darcy porous medium saturated with Newtonian fluid of variable viscosity. Seddeek and Salama [12] carried out the effects of temperature dependent viscosity and thermal conductivity with variable suction on unsteady MHD convective heat transfer past a vertical moving porous plate. Considering the internal heat generation/absorption and suction/blowing effects the flow and heat transfer of a fluid through a porous medium over a stretching surface was investigated by Cortell [13]. Kafoussis [14] calculated local similarity solution for mixed convective and mass transfer flow past a semi-infinite vertical plate. Alam et al. [15] analyzed the effects of variable chemical reaction and variable electric conductivity on free convective flow with heat and mass transfer over a stretching sheet considering Dufour and Soret effects. Convection heat transfer of non-Newtonian power-law fluids past a power-law stretched sheet with surface heat flux under the influence of magnetic field and suction/injection was performed by Chen [16]. Anghel et al. [17] studied Dufour and Soret effects on free convection boundary layer over a vertical surface embedded in a porous medium. Alam et al. [18] investigated the mixed convection and mass transfer flow past a vertical porous plate in a porous medium in the presence of heat generation and thermal diffusion. Rahman et al. [19] presented the effects of Reynolds and Prandtl numbers on MHD mixed convection in a lid-driven cavity along with joule heating and a centered heat conducting circular block. Ahammad et al. [20] investigated the influence of inlet and outlet port in a ventilated cavity containing a heat generating square block. They

found that the location of inlet and exit plays a significant role on both the flow and thermal fields. Alam et al. [21] studied the thermophoretic particle deposition on unsteady hydromagnetic radiative heat and mass transfer flow along an infinite inclined permeable surface with viscous dissipation and joule heating. Esmaeil Khaje et al. [22] analyzed the effect of heat generation on free convection boundary-layer flow over an arbitrarily impermeable inclined surface in a saturated porous medium.

Very recently Ahammad, M.U.,Obayedullah Md. And Rahman, M.M.[23] have studied on MHD free convection flow along a vertical porous plate embedded in a porous medium with magnetic field and heat generation.

In all the aforementioned analysis the combined effects of the temperature dependent viscosity and thermal conductivity and viscous dissipation with magnetic field and heat generation have not been studied. In most of the earlier studies, the viscosity and thermal conductivity of the fluid were assumed to be constant. However it is known from the work of Herwig and Gerstem[24] that these properties may change with temperature, especially the fluid viscosity. The concept of variable viscosity was first introduced by Ling and Dybbs [25], on their study of forced convective flow in porous medium. When the effects of variable viscosity and thermal conductivity are taken into account, the flow characteristics are significantly changed compared to the constant property case. In the present study an attempt has been made to incorporate the combined effects of the variable viscosity, variable thermal conductivity and viscous dissipation on MHD free convection flow along a vertical porous plate embedded in a porous medium with magnetic field and heat generation. . Following Lai and Kulacki[26], the fluid viscosity and thermal conductivity are assumed to vary as an inverse linear functions of temperature.

II. Mathematical Analysis

Consider a steady two-dimensional heat transfer flow of a viscous and incompressible electrically conducting fluid along a vertical stretching permeable sheet in a porous medium with viscous dissipation and heat generation. The flow is taken in the *x*-direction, which is along the plate in the upward direction while the *y*-axis is taken to be normal to the plate. The velocity components u and v are taken in x and y directions respectively. A transverse uniform magnetic field of strength B_0 is applied in the *y*-direction and it produces magnetic force $\vec{F} = \dfrac{\sigma B_0^2}{\rho}$ in *x*-direction, where σ is the electrical conductivity.

The analysis is based on the following assumptions:

- The fluid has constant physical properties, except for the fluid viscosity and thermal conductivity, which are assumed to be inverse linear functions of temperature.
- The magnetic Reynolds number is assumed to be small so that the induced magnetic field is negligible.
- Since the induced magnetic field is assumed to be negligible and as B_0 is independent of time, *curl* $\vec{E} = \vec{0}$. Also *div* $\vec{E}$ = 0 in the absence of surface charge density. Hence $\vec{E} = \vec{0}$ is assumed.
- The energy equation involves the viscous dissipation term and heat source term.
- The effect of the joule dissipation are assumed to be negligible in the energy equation.
- In the beginning, the plate and the fluid are taken into account at the same temperature *T* while *C* is the concentration all over the place in the fluid. The surface of the plate is maintained at a uniform constant temperature *Tw* (> *T*∞) and concentration *Cw* (> *C*∞), where *T*∞ and *C*∞ respectively are the corresponding values sufficiently far away from the flat surface.

Using the Darcy-Forchhemier model together with the Boussnesq's and the above boundary-layer approximations the current problem is governed by the continuity, momentum, energy and concentration equations respectively are given by:

$$\frac{\partial u}{\partial x} + \frac{\partial v}{\partial y} = 0 \qquad \ldots(1)$$

$$u\frac{\partial u}{\partial x} + v\frac{\partial u}{\partial y} = \frac{1}{\rho_\infty}\frac{\partial}{\partial y}\left(\mu\frac{\partial u}{\partial y}\right) + g\beta\left(T - T_\infty\right) - \frac{\sigma B_o^2}{\rho_\infty}u - \frac{\mu}{\rho_\infty k}u - \frac{b}{k}u^2 \qquad \ldots(2)$$

$$\rho_\infty c_p\left(u\frac{\partial T}{\partial x} + v\frac{\partial T}{\partial y}\right) = \frac{\partial}{\partial y}\left(\lambda\frac{\partial T}{\partial y}\right) + Q_o\left(T - T_\infty\right) + \mu\left(\frac{\partial u}{\partial y}\right)^2 \qquad \ldots(3)$$

$$u\frac{\partial C}{\partial x} + v\frac{\partial C}{\partial y} = \frac{\partial}{\partial y}\left(D_m\frac{\partial C}{\partial y}\right) \qquad \ldots(4)$$

where ρ_∞ is the fluid density in the free stream, μ is the viscosity of the fluid, g is the acceleration due to gravity, β is the volumetric coefficient of thermal expansion, T is the fluid temperature inside the boundary layer, T_∞ is the fluid temperature in the free-stream, σ is the electrical conductivity, k is the Darcy permeability constant, b is the stretching rate, c_p is the specific heat at constant pressure, λ is the thermal conductivity of fluid, Q_0 is the volumetric rate of heat generation, C is the concentration of the fluid within the boundary layer, D_m is the molecular diffusivity of the species concentration.

The boundary conditions are given as:

$$u = bx, \quad v = v_w(x), \quad T = T_w, \quad C = C_w, \quad \text{at} \quad y = 0, \qquad \text{...(5a)}$$

$$u = 0, \qquad T = T_\infty, \quad C = C_\infty, \quad \text{as} \quad y \to \infty. \qquad \text{...(5b)}$$

where $v_w(x)$ represents the permeability of the porous surface where its sign indicates suction (< 0) or injection (> 0).

The velocity components along the axes can be expressed as:

$$u = \frac{\partial \psi}{\partial y}, \qquad v = -\frac{\partial \psi}{\partial x} \qquad \text{...(6)}$$

where ψ is the stream function such that the continuity equation is satisfied.

Now we introduce the following similarity transformations[27] with dimensionless stream function $f(\eta)$ given by:

$$\psi(x, y) = (b\upsilon_\infty)^{1/2} x f(\eta), \quad \eta = (b/\upsilon_\infty)^{1/2} y \qquad \text{...(7a)}$$

$$\theta(\eta) = \frac{T - T_\infty}{T_w - T_\infty}, \qquad \varphi(\eta) = \frac{C - C_\infty}{C_w - C_\infty} \qquad \text{...(7b)}$$

where υ_∞ is the kinematic viscosity of the fluid in the free stream.

From Eqs. (6) and (7a), the velocity components become:

$$u = bxf', \qquad v = -(b\upsilon_\infty)^{1/2} f \qquad \text{...(8)}$$

where the prime $(')$ denotes derivative with respect to η.

It is known that, viscosity and thermal conductivity are inverse linear functions of temperature, following Lai and Kulacki[26], we assume

$$\frac{1}{\mu} = \frac{1}{\mu_\infty}\left[1 + \delta\left(T - T_\infty\right)\right] \qquad \text{...(9)}$$

or, $$\frac{1}{\mu} = \alpha\left(T - T_r\right),$$

where $\alpha = \dfrac{\delta}{\mu_\infty}$ and $T_r = T_\infty - \dfrac{1}{\delta}$

And

$$\frac{1}{\lambda} = \frac{1}{\lambda_\infty}\left[1 + \xi\left(T - T_\infty\right)\right] \qquad \text{...(10)}$$

or, $$\frac{1}{\lambda} = \zeta\left(T - T_c\right),$$

where $\zeta = \dfrac{\xi}{\lambda_\infty}$ and $T_c = T_\infty - \dfrac{1}{\xi}$

Where α , ζ , T_r and T_c are constants and their values depend on the reference state and thermal properties of the fluid i.e., υ (kinematic viscosity) and λ (thermal conductivity). In general α >0 for liquids and α <0 for gases. The non-dimensional form of viscosity and thermal conductivity parameters θ_r and θ_c can be written as,

$$\theta_r = \frac{T_r - T_\infty}{T_w - T_\infty} \quad \text{and} \quad \theta_c = \frac{T_c - T_\infty}{T_w - T_\infty} \qquad ...(11)$$

Substituting Eqs. (7a)-(11) with the boundary conditions given in Eqs.(5a)-(5b) in the Eqs. (2)-(4), we have

$$\frac{\theta_r}{\theta - \theta_r} f''' - ff'' + f'^2 + \frac{Fs}{Da} f'^2 + Mf' + \frac{1}{Da\,\mathrm{Re}} f' - \frac{\theta_r}{(\theta - \theta_r)^2}\theta' f' - \gamma\theta = 0 \qquad ...(12)$$

$$\frac{\theta_c}{\theta - \theta_c}\theta'' - \frac{\theta_c}{(\theta - \theta_c)^2}\theta'^2 - \mathrm{Pr}\, f\theta' - \mathrm{Pr}\, Q\theta + \mathrm{Pr}\, Ec \frac{\theta_r}{\theta - \theta_r} f''^2 = 0 \qquad ...(13)$$

$$\frac{\theta_r}{\theta - \theta_r}\varphi'' - \frac{\theta_r}{(\theta - \theta_r)^2}\theta'\varphi' - Scf\varphi' = 0 \qquad ...(14)$$

where the dimensionless parameters are defined as follows:

$\gamma = \frac{Gr}{\mathrm{Re}^2}$ is the temperature buoyancy parameter, Gr is the Grashof number, $M = \frac{\sigma B_0^2}{\rho_\infty b}$ is the magnetic field parameter, $Da = \frac{k}{x^2}$ is the Darcy number, $\mathrm{Re} = \frac{u_w(x)x}{\upsilon_\infty}$ is the Reynolds number, υ_∞ is the kinematic viscosity in the free stream, $Fs = \frac{b}{x}$ is the Forchhemier number, $\mathrm{Pr} = \frac{\upsilon_\infty \rho_\infty c_p}{\lambda_\infty}$ is the Prandtl number, $Ec = \frac{u_0^2}{c_p(T_w - T_\infty)}$ is the Eckert number, $Q = \frac{Q_0}{b\rho_\infty c_p}$ is the heat generating parameter, Q_0 is the volumetric rate of heat generation, $Sc = \frac{\upsilon}{Dm}$ is the Schmidt number.

The boundary conditions (5a) and (5b) become:

$$f = f_w, \quad f' = 1, \quad \theta = 1, \quad \varphi = 1 \quad \text{at} \quad \eta = 0 \qquad ...(15a)$$

$$f' = 0, \quad \theta = 0, \quad \varphi = 0 \quad \text{as} \quad \eta \to \infty \qquad ...(15b)$$

where $f_w = -\frac{v_w}{(b\upsilon_\infty)^{1/2}}$ is the dimensionless wall mass transfer coefficient such that f_w >0 indicates wall suction and $f_w < 0$ indicates wall injection.

For the present problem the local skin-friction coefficient, the local Nusselt number and the local Sherwood number are the parameters of engineering interest which are given respectively as below:

$C_f = \frac{2\tau_w}{\rho_\infty u_0^2}$, where $\tau_w = \mu \frac{\partial u}{\partial y}\Big)_{y=0}$ is the shearing stress.

$$\Rightarrow C_f = -\frac{2\theta_r}{\theta - \theta_r}\mathrm{Re}^{-1/2} f''(0);$$

$$Nu = \frac{-x}{T_w - T_\infty} \cdot \frac{\partial T}{\partial y}\Bigg)_{y=0}$$

$$\Rightarrow Nu = -\mathrm{Re}^{1/2}\,\theta'(0)$$

And

$$Sh = -\frac{Js}{u_0(C_w - C_\infty)}, \qquad \text{where} \quad Js = -Dm\frac{\partial C}{\partial y}\Bigg)_{y=0}$$

$$\Rightarrow Sh = -\mathrm{Re}^{-1/2}\,Sc^{-1}\frac{\theta_r}{\theta - \theta_r}\varphi'(0).$$

The governing Eqs.(12)-(14) with boundary conditions given in Eqs.(15a)-(15b) are solved numerically by using Runge-Kutta Shooting method.

III. Results And Discussion

The system of differential equations (12)-(14) governed by the boundary conditions .(15a)-(15b) are solved numerically by an efficient numerical technique based on the fourth order Runge-Kutta Shooting method. The numerical method can be programmed and applied easily. It is experienced that the convergence of the iteration process is quite rapid. The numerical computations have been carried out for various parameters involved in the problem viz., viscosity parameter θ_r, thermal conductivity parameter θ_c, magnetic parameter *M* and Eckert number *Ec*. In order to illustrate the results graphically, the numerical values of dimensionless velocity $f'(\eta)$, dimensionless temperature $\theta(\eta)$ and dimensionless concentration $\varphi(\eta)$ are plotted from Fig.1 to Fig.17.

For various values of the viscosity parameter θ_r, the velocity profiles are plotted in Fig. 1 and Fig.2. It can be seen that as θ_r increases, the velocity decreases.

In Fig.3 we are observing that the effect of viscosity parameter θ_r on the temperature profile. It is observed that the temperature increases as the viscosity parameter increases.

Fig.4 and Fig.5 represent concentration profiles for various values of viscosity parameter θ_r. In both the cases, concentration decreases with increasing θ_r.

From the Figs.(6-11) it is seen that velocity, temperature and concentration profiles are decreased with the thermal conductivity parameter θ_c increases.

The impacts of the Magnetic parameter *M* on the velocity, temperature and concentration profiles are very significant in practical point of view. In Figs.(12-14), the variations in velocity field, temperature distribution and concentration profiles for several values of *M* are presented. In Fig.12 the dimensionless velocity $f'(\eta)$ decreases with *M* increases. Accordingly, the thickness of the momentum boundary layer decreases. This happens due to the Lorentz force arising from the interaction of magnetic and electric fields during the motion of the electrically conducting fluid. To reduce momentum boundary layer thickness the general Lorentz force retards the fluid motion in the boundary layer region. On the other hand, from Fig.13 and Fig.14, it is noticed that the temperature $\theta(\eta)$ and concentration $\varphi(\eta)$ increase with increasing values of *M*.

The effect of Eckert number *Ec* on the velocity, temperature and concentration profiles are depicted from Fig.15 to Fig.17. It is observed that velocity, temperature and concentration profiles increase with the increase of the *Ec*.

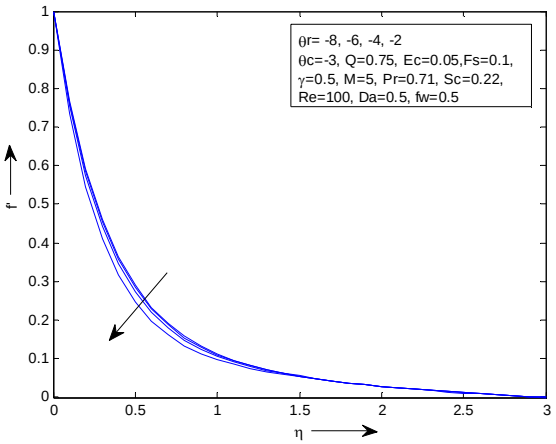

Fig.1: Velocity profile for different Θr

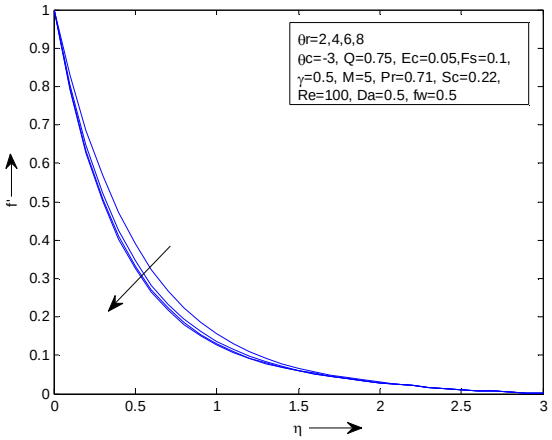

Fig.2: Velocity profile for different Θr

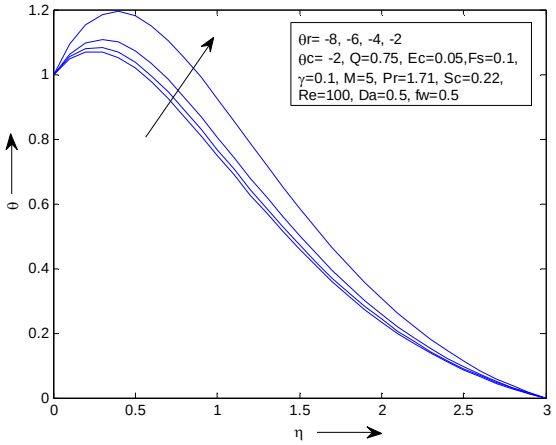

Fig.3: Temperature profile for different Θr

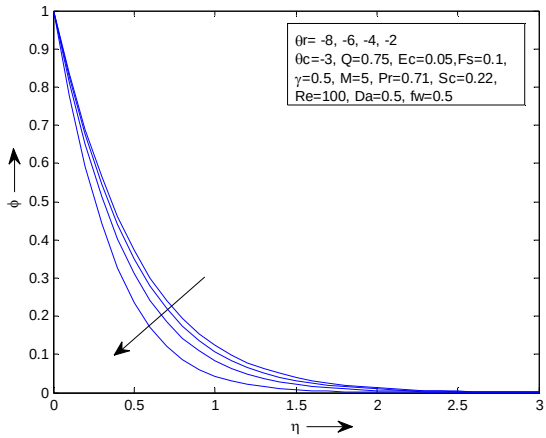

Fig.4: Concentration profile for different Θr

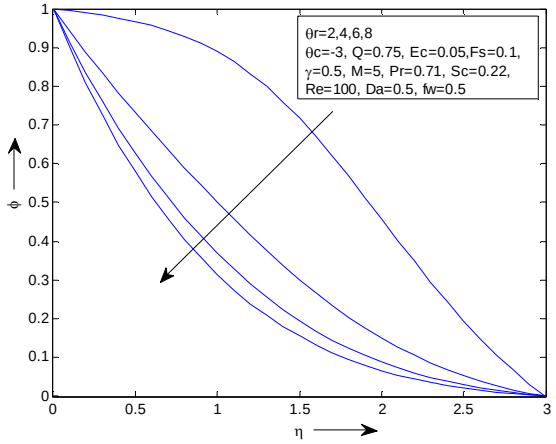

Fig.5: Concentration profile for different Θr

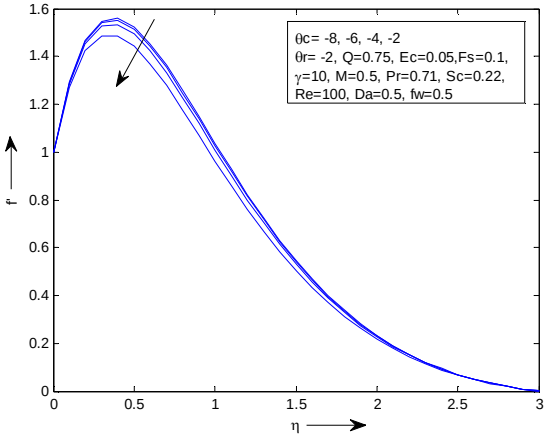

Fig.6: Velocity profile for different Θc

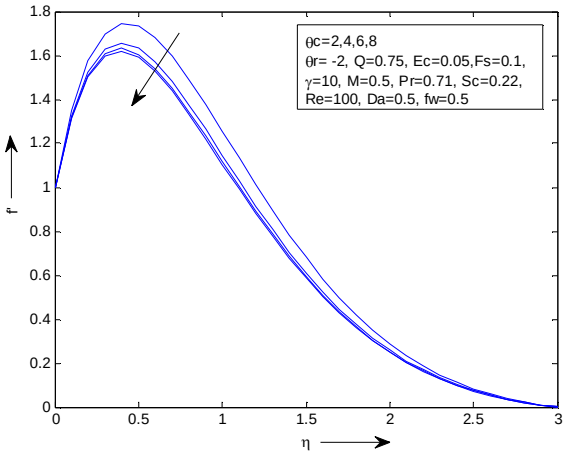

Fig.7: Velocity profile for different Θc

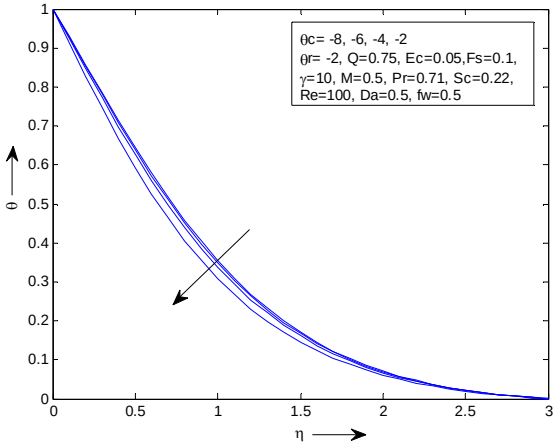

Fig.8: Temperature profile for different Θc

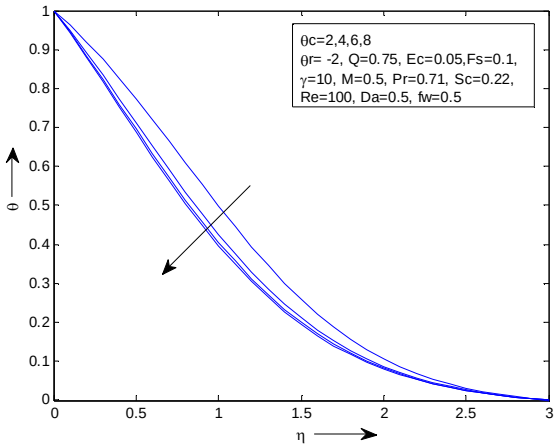

Fig.9: Temperature profile for different Θc

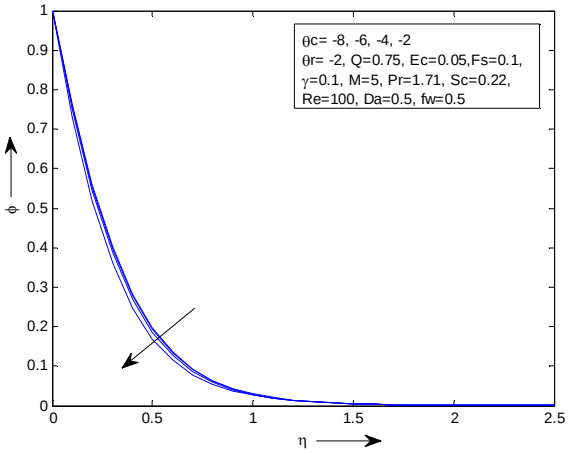

Fig.10: Concentration profile for different Θc

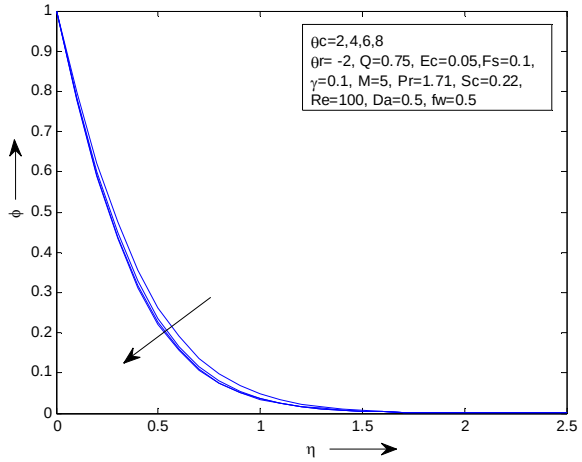

Fig.11: Concentration profile for different Θc

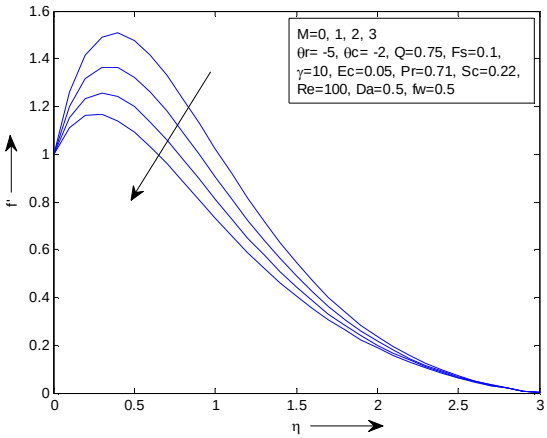

Fig.12: Velocity profile for different M

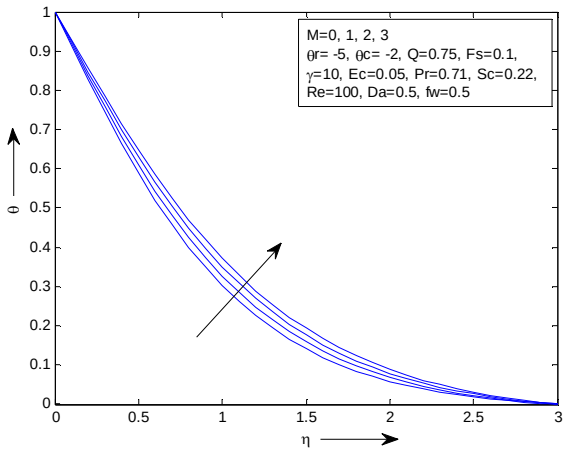

Fig.13: Temperature profile for different M

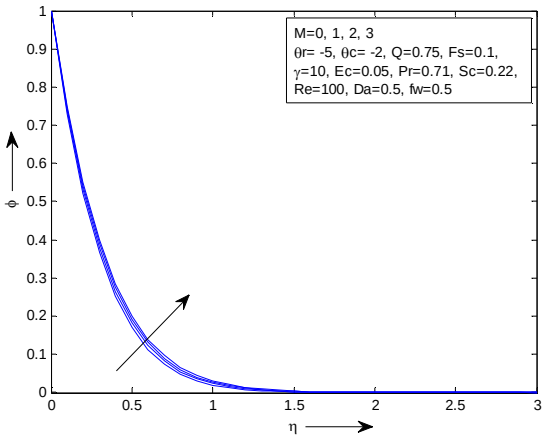

Fig.14: Concentration profile for different M

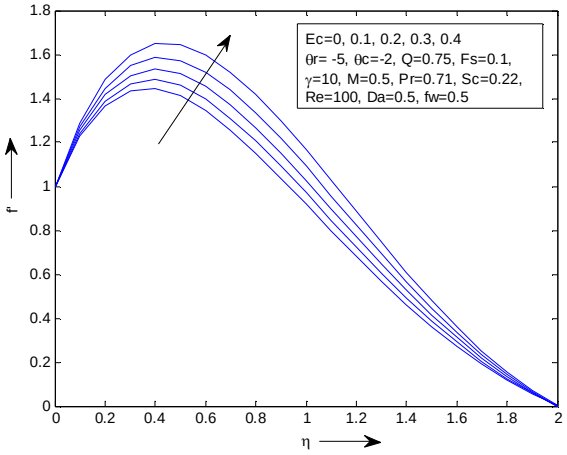

Fig.15: Velocity profile for different Ec

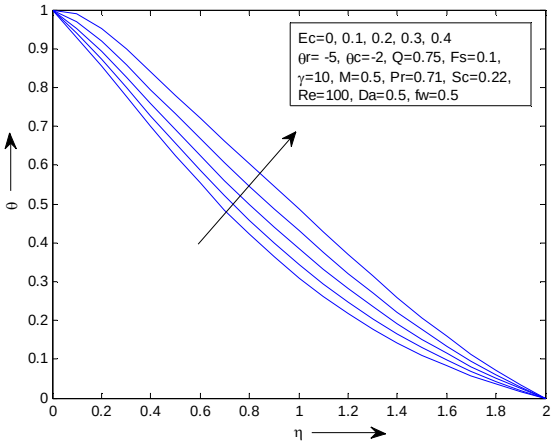

Fig.16: Temperature profile for different Ec

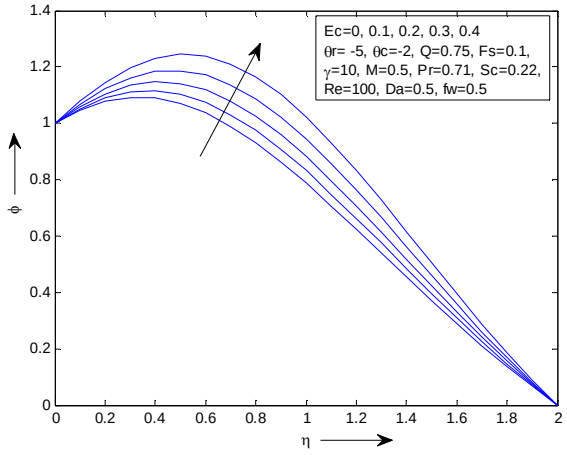

Fig.17: Concentration profile for different Ec

The missing values of $f''(0), \theta'(0)$ and $\varphi'(0)$ are estimated from Table 1 to Table 8 for various values of the viscosity parameter θr, thermal conductivity parameter θc, magnetic parameter *M* and Eckert number *Ec*.

TABLE 1:

Estimated missing values of $f''(0), \theta'(0)$ and $\varphi'(0)$ for various θr, M and θc = -2, Pr=0.71, Fs=0.10, Da=0.5, γ =10, Sc=0.22, Re=100, Ec=0.1, Q=0.75, fw=0.1

M →	1			2			3		
$\theta r \downarrow$	$f''(0)$	$\theta'(0)$	$\varphi'(0)$	$f''(0)$	$\theta'(0)$	$\varphi'(0)$	$f''(0)$	$\theta'(0)$	$\varphi'(0)$
-9	2.40793	-0.54098	0.331183	1.875043	-0.53407	0.316099	1.40799	-0.52015	0.302676
-8	2.433339	-0.54151	0.368889	1.895884	-0.53461	0.353449	1.424893	-0.52067	0.339661
-7	2.465767	-0.54219	0.416689	1.922468	-0.5353	0.400795	1.446443	-0.52133	0.386539
-6	2.508589	-0.5431	0.479257	1.957556	-0.53622	0.462767	1.474865	-0.52221	0.447889
-5	2.567773	-0.54438	0.564678	2.006011	-0.53748	0.547369	1.514082	-0.52342	0.531626
-4	2.654946	-0.54628	0.688241	2.07731	-0.53935	0.669736	1.571715	-0.52518	0.652714
-3	2.796245	-0.54943	0.882728	2.192709	-0.54239	0.862324	1.66483	-0.52801	0.843225

TABLE 2:

Estimated missing values of $f''(0), \theta'(0)$ and $\varphi'(0)$ for various θr, M and θc = -2, Pr=0.71, Fs=0.10, Da=0.5, γ =10, Sc=0.22, Re=100, Ec=0.1, Q=0.75, fw=0.1

M →	1			2			3		
$\theta r \downarrow$	$f''(0)$	$\theta'(0)$	$\varphi'(0)$	$f''(0)$	$\theta'(0)$	$\varphi'(0)$	$f''(0)$	$\theta'(0)$	$\varphi'(0)$
2	1.049767	-0.5182	-1.91728	0.743004	-0.50637	-1.91682	0.472503	-0.48967	-1.9168
3	1.481872	-0.52427	-1.16921	1.107971	-0.5151	-1.17228	0.778655	-0.5002	-1.17461
4	1.676132	-0.52732	-0.83807	1.270345	-0.51898	-0.84334	0.913262	-0.50458	-0.84746
5	1.78721	-0.52917	-0.6517	1.362788	-0.52121	-0.65833	0.989518	-0.50702	-0.66365
6	1.859227	-0.53041	-0.53228	1.42258	-0.52267	-0.53984	1.038705	-0.50858	-0.54598

TABLE 3:

Estimated missing values of $f''(0), \theta'(0)$ and $\varphi'(0)$ for various θc, M and θr = -5, Pr=0.71, Fs=0.10, Da=0.5, γ =10, Sc=0.22, Re=100, Ec=0.1, Q=0.75, fw=0.1

M→	1			2			3		
$\theta c \downarrow$	$f''(0)$	$\theta'(0)$	$\varphi'(0)$	$f''(0)$	$\theta'(0)$	$\varphi'(0)$	$f''(0)$	$\theta'(0)$	$\varphi'(0)$
-6	2.683353	-0.47726	0.616813	2.107552	-0.47298	0.594991	1.602922	-0.4626	0.575156
-5	2.670688	-0.48443	0.610889	2.096426	-0.47989	0.589588	1.593189	-0.46914	0.570225
-4	2.652203	-0.49496	0.602337	2.080188	-0.49005	0.581786	1.578983	-0.47874	0.563102
-3	2.622664	-0.51201	0.588904	2.054237	-0.50644	0.569519	1.556278	-0.49422	0.551894
-2	2.567773	-0.54438	0.564678	2.006011	-0.53748	0.547369	1.514082	-0.52342	0.531626

TABLE 4:

Estimated missing values of $f''(0), \theta'(0)$ and $\varphi'(0)$ for various θc, M and θr = -5, Pr=0.71, Fs=0.10, Da=0.5, γ =10, Sc=0.22, Re=100, Ec=0.1, Q=0.75, fw=0.1

M →	1			2			3		
$\theta c \downarrow$	$f''(0)$	$\theta'(0)$	$\varphi'(0)$	$f''(0)$	$\theta'(0)$	$\varphi'(0)$	$f''(0)$	$\theta'(0)$	$\varphi'(0)$
2	3.027909	-0.29879	0.801342	2.410217	-0.29887	0.76232	1.867706	-0.29555	0.726929
3	2.918992	-0.35192	0.737711	2.31454	-0.35108	0.704815	1.783995	-0.34607	0.674955
4	2.871974	-0.37577	0.711859	2.273238	-0.37442	0.681396	1.747864	-0.36853	0.653737
5	2.845619	-0.38939	0.697767	2.250088	-0.38771	0.668617	1.727612	-0.3813	0.642144
6	2.828735	-0.39821	0.688884	2.235257	-0.39631	0.660555	1.714638	-0.38954	0.634826

TABLE 5:

Estimated missing values of $f''(0), \theta'(0)$ and $\varphi'(0)$ for various θr, Ec and θc = -2, Pr=0.71, Fs=0.10, Da=0.5, γ =10, Sc=0.22, Re=100, M=0.5, Q=0.75, fw=0.1

Ec→	0.1			0.2			0.3		
$\theta r \downarrow$	$f''(0)$	$\theta'(0)$	$\varphi'(0)$	$f''(0)$	$\theta'(0)$	$\varphi'(0)$	$f''(0)$	$\theta'(0)$	$\varphi'(0)$
-6	2.815467	-0.54229	0.488363	2.955892	-0.37365	0.549906	3.11962	-0.16689	0.623048
-5	2.880695	-0.54354	0.574166	3.023067	-0.37371	0.634891	3.188849	-0.16593	0.706526
-4	2.976813	-0.54541	0.698276	3.12194	-0.374	0.757572	3.290569	-0.16494	0.82672
-3	3.132711	-0.54856	0.893603	3.282012	-0.37494	0.95009	3.454811	-0.16436	1.014649
-2	3.430126	-0.55486	1.245536	3.586387	-0.3782	1.295411	3.765688	-0.16634	1.349967

TABLE 6:

Estimated missing values of $f''(0), \theta'(0)$ and $\varphi'(0)$ for various θr, Ec and θc = -2, Pr=0.71, Fs=0.10, Da=0.5, γ =10, Sc=0.22, Re=100, M=0.5, Q=0.75, fw=0.1

Ec→	0.1			0.2			0.3		
$\theta r \downarrow$	$f''(0)$	$\theta'(0)$	$\varphi'(0)$	$f''(0)$	$\theta'(0)$	$\varphi'(0)$	$f''(0)$	$\theta'(0)$	$\varphi'(0)$
2	1.219808	-0.52117	-1.9177	1.298827	-0.41231	-1.88972	1.388409	-0.27875	-1.85465
3	1.689299	-0.52545	-1.16724	1.787785	-0.39276	-1.11882	1.90194	-0.22787	-1.05677
4	1.901393	-0.52788	-0.83479	2.008655	-0.38606	-0.77953	2.133754	-0.2095	-0.70903
5	2.022911	-0.52944	-0.64764	2.135092	-0.38287	-0.58937	2.266238	-0.20043	-0.5154
6	2.101784	-0.53051	-0.5277	2.217097	-0.38107	-0.46785	2.352051	-0.19512	-0.39219

TABLE 7:

Estimated missing values of $f''(0), \theta'(0)$ and $\varphi'(0)$ for various θc, Ec and θr = -5, Pr=0.71, Fs=0.10, Da=0.5, γ =10, Sc=0.22, Re=100, M=0.5, Q=0.75, fw=0.1

Ec →	0.1			0.2			0.3		
$\theta c \downarrow$	$f''(0)$	$\theta'(0)$	$\varphi'(0)$	$f''(0)$	$\theta'(0)$	$\varphi'(0)$	$f''(0)$	$\theta'(0)$	$\varphi'(0)$
-6	3.003626	-0.4758	0.628714	3.133208	-0.33362	0.689403	3.280809	-0.16365	0.759621
-5	2.990155	-0.48302	0.62251	3.121139	-0.33794	0.683215	3.270695	-0.16408	0.7536
-4	2.970494	-0.49364	0.613559	3.103523	-0.34428	0.674279	3.255949	-0.16463	0.744904
-3	2.939076	-0.51084	0.599502	3.075372	-0.35448	0.660237	3.232426	-0.16531	0.73123
-2	2.880695	-0.54354	0.574166	3.023067	-0.37371	0.634892	3.188849	-0.16593	0.706526

TABLE 8:

Estimated missing values of $f''(0), \theta'(0)$ and $\varphi'(0)$ for various θc, Ec and θr = -5, Pr=0.71, Fs=0.10, Da=0.5, γ =10, Sc=0.22, Re=100, M=0.5, Q=0.75, fw=0.1

Ec →	0.1			0.2			0.3		
$\theta c \downarrow$	$f''(0)$	$\theta'(0)$	$\varphi'(0)$	$f''(0)$	$\theta'(0)$	$\varphi'(0)$	$f''(0)$	$\theta'(0)$	$\varphi'(0)$
2	3.370119	-0.29683	0.822437	3.461834	-0.22149	0.881223	3.559771	-0.13697	0.945267
3	3.254265	-0.34995	0.755529	3.357879	-0.25588	0.815293	3.470772	-0.14833	0.88167
4	3.204253	-0.37384	0.728377	3.31303	-0.27101	0.788441	3.432593	-0.15244	0.855705
5	3.176221	-0.38749	0.713584	3.287896	-0.27957	0.773787	3.411254	-0.15453	0.84152
6	3.158262	-0.39633	0.704262	3.271796	-0.28509	0.764545	3.397607	-0.15578	0.832568

Table 9 to Table 16 demonstrates the effects of various parameters on coefficient of skin-friction C_f, which represent the plate shearing stress, heat transfer coefficient in term of Nusselt number Nu and mass transfer in term of Sherwood number Sh.

From Table 9 and Table 10 it is observed that the coefficient of skin friction decreases for increasing values of the viscosity parameter θ_r when θ_r is negative and increases when θ_r is positive. Nusselt number and Sherwood number both are increased as θ_r increases, whereas Nusselt number decreases for increasing values of magnetic parameter M in both θ_r positive and negative. But Sherwood number decreases as M increases when θ_r is negative while that of decreases when θ_r is positive.

It is observed from Table 11 and Table 12 that rate of skin-friction and mass transfer retard due to increase of both thermal conductivity parameter θ_c and magnetic parameter M whereas rate of heat transfer enhances due to increase of θ_c and retards due to increase of M.

Table 13 and Table 14 indicates the influence of Eckert number Ec on coefficient of the skin-friction, the rate of heat transfer and the rate of mass transfer for various values of the viscosity parameter θ_r. It is seen that that the skin-friction coefficient and mass transfer increase due to raise the Eckert number but the rate of heat transfer decreases with it.

Table 15 and Table 16 reveal that the enhancement of the Eckert number makes raise skin-friction coefficient and mass transfer whereas heat transfer decreases. It is observed for various values of thermal conductivity parameter θ_c.

TABLE 9:

Effects of θr and M on local skin-friction coefficient(C_f), local Nusselt number(Nu) and local Sherwood number(Sh) for θc = -2, Pr=0.71, Fs=0.10, Da=0.5, γ =10, Sc=0.22, Re=100, Ec=0.1, Q=0.75, fw=0.1

M →	1			2			3		
$\theta r \downarrow$	C_f	Nu	Sh	C_f	Nu	Sh	C_f	Nu	Sh
-6	0.430044	5.431017	0.186723	0.335581	5.362154	0.180299	0.252834	5.222097	0.174502
-5	0.427962	5.443748	0.213893	0.334335	5.374798	0.207337	0.252347	5.234153	0.201374
-4	0.424791	5.462793	0.25027	0.33237	5.39348	0.24354	0.251474	5.2518	0.237351
-3	0.419437	5.494335	0.30093	0.328906	5.423878	0.293974	0.249725	5.280119	0.287463
-2	0.408739	5.556371	0.373707	0.321619	5.481991	0.366487	0.24552	5.333041	0.359516

TABLE 10:

Effects of θr and M on local skin-friction coefficient(C_f), local Nusselt number(Nu) and local Sherwood number(Sh) for θc = -2, Pr=0.71, Fs=0.10, Da=0.5, γ =10, Sc=0.22, Re=100, Ec=0.1, Q=0.75, fw=0.1

M →	1			2			3		
$\theta r \downarrow$	C_f	Nu	Sh	C_f	Nu	Sh	C_f	Nu	Sh
2	0.419907	5.181954	-1.74298	0.297202	5.063665	-1.74256	0.189001	4.896646	-1.74255
3	0.444562	5.242721	-0.79719	0.332391	5.150975	-0.79928	0.233596	5.002032	-0.80087
4	0.446969	5.273176	-0.50792	0.338759	5.189756	-0.51111	0.243536	5.045761	-0.51361
5	0.446803	5.291688	-0.37029	0.340697	5.21211	-0.37405	0.247379	5.070167	-0.37708
6	0.446215	5.304128	-0.29034	0.341419	5.226702	-0.29446	0.249289	5.085809	-0.29781

TABLE 11:

Effects of θc and M on local skin-friction coefficient(C_f), local Nusselt number(Nu) and local Sherwood number(Sh) for θr = -5, Pr=0.71, Fs=0.10, Da=0.5, γ =10, Sc=0.22, Re=100, Ec=0.1, Q=0.75, fw=0.1

M→	1			2			3		
$\theta c \downarrow$	C_f	Nu	Sh	C_f	Nu	Sh	C_f	Nu	Sh
-6	0.447225	4.772618	0.233641	0.351259	4.729809	0.225375	0.267154	4.625959	0.217862
-5	0.445115	4.844247	0.231397	0.349404	4.798909	0.223329	0.265532	4.6914	0.215994
-4	0.442034	4.949616	0.228158	0.346698	4.900448	0.220373	0.263164	4.787436	0.213296
-3	0.437111	5.120069	0.22307	0.342373	5.064414	0.215727	0.25938	4.942213	0.209051
-2	0.427962	5.443748	0.213893	0.334335	5.374798	0.207337	0.252347	5.234153	0.201373

TABLE 12:

Effects of θc and M on local skin-friction coefficient(C_f), local Nusselt number(Nu) and local Sherwood number(Sh) for θr = -5, Pr=0.71, Fs=0.10, Da=0.5, γ =10, Sc=0.22, Re=100, Ec=0.1, Q=0.75, fw=0.1

M→	1			2			3		
$\theta c \downarrow$	C_f	Nu	Sh	C_f	Nu	Sh	C_f	Nu	Sh
2	0.504652	2.987931	0.303539	0.401703	2.988666	0.288758	0.311284	2.955528	0.275352
3	0.486499	3.519219	0.279436	0.385757	3.510795	0.266975	0.297333	3.460701	0.255665
4	0.478662	3.75773	0.269644	0.378873	3.744173	0.258105	0.291311	3.685344	0.247628
5	0.47427	3.893883	0.264306	0.375015	3.8771	0.253264	0.287935	3.812974	0.243236
6	0.471456	3.982049	0.260941	0.372543	3.963066	0.25021	0.285773	3.895387	0.240464

TABLE 13:

Effects of θr and Ec on local skin-friction coefficient(C_f), local Nusselt number(Nu) and local Sherwood number(Sh) for θc = -2, Pr=0.71, Fs=0.10, Da=0.5, γ =10, Sc=0.22, Re=100, M=0.5, Q=0.75, fw=0.1

Ec →	0.1			0.2			0.3		
$\theta r \downarrow$	C_f	Nu	Sh	C_f	Nu	Sh	C_f	Nu	Sh
-6	0.482652	5.422926	0.190271	0.506724	3.736522	0.214249	0.534792	1.66892	0.242746
-5	0.480116	5.43537	0.217487	0.503845	3.737116	0.240489	0.531475	1.659315	0.267624
-4	0.47629	5.454144	0.253918	0.49951	3.739976	0.275481	0.526491	1.649444	0.300625
-3	0.469907	5.485604	0.304637	0.492302	3.749378	0.323894	0.518222	1.643609	0.345903
-2	0.45735	5.548626	0.377435	0.478185	3.782018	0.392549	0.502092	1.663348	0.409081

TABLE 14:

Effects of θr and Ec on local skin-friction coefficient(C_f), local Nusselt number(Nu) and local Sherwood number(Sh) for θc = -2, Pr=0.71, Fs=0.10, Da=0.5, γ =10, Sc=0.22, Re=100, M=0.5, Q=0.75, fw=0.1

Ec →	0.1			0.2			0.3		
$\theta r \downarrow$	C_f	Nu	Sh	C_f	Nu	Sh	C_f	Nu	Sh
2	0.487923	5.211721	-1.74336	0.519531	4.123059	-1.71793	0.555364	2.787454	-1.68604
3	0.50679	5.254478	-0.79584	0.536335	3.927613	-0.76283	0.570582	2.278698	-0.72052
4	0.507038	5.278826	-0.50593	0.535641	3.860557	-0.47244	0.569001	2.094955	-0.42971
5	0.505728	5.294369	-0.36798	0.533773	3.828735	-0.33487	0.56656	2.00426	-0.29284
6	0.504428	5.305081	-0.28784	0.532103	3.81068	-0.25519	0.564492	1.951181	-0.21392

TABLE 15:

Effects of θc and Ec on local skin-friction coefficient(C_f), local Nusselt number(Nu) and local Sherwood number(Sh) for θr = -5, Pr=0.71, Fs=0.10, Da=0.5, γ =10, Sc=0.22, Re=100, M=0.5, Q=0.75, fw=0.1

Ec →	0.1			0.2			0.3		
$\theta c \downarrow$	C_f	Nu	Sh	C_f	Nu	Sh	C_f	Nu	Sh
-6	0.500604	4.758022	0.238149	0.522201	3.336151	0.261138	0.546802	1.636484	0.287735
-5	0.498359	4.830196	0.235799	0.52019	3.379381	0.258794	0.545116	1.640768	0.285455
-4	0.495082	4.936415	0.232409	0.517254	3.442773	0.255409	0.542658	1.646249	0.282161
-3	0.489846	5.108375	0.227084	0.512562	3.544839	0.25009	0.538738	1.65308	0.276981
-2	0.480116	5.435371	0.217487	0.503845	3.737115	0.240489	0.531475	1.659314	0.267624

TABLE 16:

Effects of θc and Ec on local skin-friction coefficient(C_f), local Nusselt number(Nu) and local Sherwood number(Sh) for θr = -5, Pr=0.71, Fs=0.10, Da=0.5, γ =10, Sc=0.22, Re=100, M=0.5, Q=0.75, fw=0.1

Ec →	0.1			0.2			0.3		
$\theta c \downarrow$	C_f	Nu	Sh	C_f	Nu	Sh	C_f	Nu	Sh
2	0.561686	2.968341	0.311529	0.576972	2.214849	0.333797	0.593295	1.369686	0.358056
3	0.542377	3.499493	0.286185	0.559646	2.558794	0.308823	0.578462	1.483256	0.333966
4	0.534042	3.738371	0.2759	0.552172	2.710125	0.298652	0.572099	1.524392	0.324131
5	0.52937	3.874855	0.270297	0.547983	2.795727	0.293101	0.568542	1.54525	0.318758
6	0.526377	3.963287	0.266766	0.545299	2.850871	0.2896	0.566268	1.557759	0.315367

IV. CONCLUSIONS

The combined effects of the variable viscosity, thermal conductivity and viscous dissipation on MHD free convection flow along a vertical porous plate have been studied numerically. From the present investigation the following conclusions were made:

- When the effects of variable viscosity and thermal conductivity are taken into account, the flow characteristics are significantly changed compared to the constant property case.
- Velocity decreases with the increase in the viscosity parameter θr , thermal conductivity parameter θc and magnetic parameter *M*, while that of increases with increase of Eckert number *Ec*.
- Temperature increases when the viscosity parameter θr , magnetic parameter *M* and Eckert number *Ec* are increased. But temperature decreases when thermal conductivity parameter θc is increased.
- Viscosity parameter and thermal conductivity parameter retard the concentration profile while that of magnetic parameter and Eckert number enhance it.

- Coefficient of skin-friction decreases for increasing values of the magnetic parameter, thermal conductivity parameter, and negative values of viscosity parameter while that of increases for increasing values of the Eckert number and positive values of viscosity parameter.
- Rate of heat transfer enhances due to increase of viscosity parameter and thermal conductivity parameter, but retards due to increase of magnetic parameter and Eckert number.
- Rate of mass transfer increases with the increase in the viscosity parameter and Eckert number, but decreases with increase of thermal conductivity parameter.

ACKNOWLEDGMENT

We are thankful to the reviewers for their valuable suggestions to enhance the quality of the article.

REFERENCES

[1] Raptis A. and Perdikis C., 2006. Viscous flow over a non-linearly stretching sheet in the presence of a chemical reaction and magnetic field, International Journal of Non-linear Mechanics, **41**(4): 527-529.

[2] Samad M.A., Karim M. E. and Mohammad D., 2010. Free convection flow through a porous medium with thermal radiation, viscous dissipation and variable suction in presence of magnetic field, The Bangladesh Journal of Scientific Research, **23**(1): 61-72.

[3] Postelnicu A., 2004. Influence of a magnetic field on heat and mass transfer by natural convection from vertical surfaces in porous media considering Soret and Dufour effects, Int. J. Heat Mass Transfer, **47**: 1467-1472.

[4] Ahammad M. U. and Shirazul Hoque Mollah Md., 2011. Numerical study of MHD free convection flow and mass transfer over a stretching sheet considering Dufour & Soret effects in the presence of magnetic Field, International Journal of Engineering & Technology IJET-IJENS, **11**(5): 4-11.

[5] Lykoudis P. S., 1962. Natural convection of an electrically conducting fluid in the presence of a magnetic field, Int. J. Heat Mass Transfer, **5**: 23-34.

[6] Gupta A. S., 1961. Steady and transient free convection of an electrically conducting fluid from a vertical plate in the presence of magnetic field, Appl. Sci. Res., **9A**: 319-333.

[7] Ravikumar V., Raju M.C., Raju G.S.S. and Chamkha A.J., 2013. MHD double diffusive and chemically reactive flow through porous medium bounded by two vertical plates, International Journal of Energy & Technology, **5(7)**: 1–8.

[8] Alam M. S. and Rahman M. M., 2006. Dufour and Soret Effects on Mixed Convection Flow Past a Vertical Porous Flat Plate with Variable Suction, Nonlinear Analysis: Modelling and Control, **11**(1): 3–12.

[9] Alam M.A., Alim Md. and Chowdhury M.K., 2007. Viscous Dissipation Effects on MHD Natural Convection Flow over a Sphere in the Presence of Heat Generation, Nonlinear Analysis: Modelling and Control, 1**2**(4): 447–459.

[10] Sattar, M. A. and Kalim, H. (1996): Unsteady Free Convection Interaction with Thermal Radiation in a Boundary Layer Flow Past a Vertical Porous Plate. *J. Math. Phys. Sci*., vol.30(1), pp.25-37.

[11] Kairi R. R. and Murthy P.V.S.N., 2013. Soret effect on free convection from a melting vertical surface in a non-Darcy porous medium, Journal of Porous Media, 16(2): 97-104.

[12] Seddeek, M. A. and Salama, F. A. (2007). The effects of temperature dependent viscosity and thermal conductivity on unsteady MHD convective heat transfer past a semi-infinite vertical porous moving plate with variable suction. Computational Materials Science, Vol. 40(2), pp. 186-192.

[13] Cortell R, 2005. Flow and heat transfer of a fluid through a porous medium over a stretching surface with internal heat generation/absorption and suction/blowing, Fluid Dyn. Res., **37**: 231-245.

[14] Kafoussis N.G., 1990. Local similarity solution for combined free-forced convective and mass transfer flow past a semi-infinite vertical plate, Int. J. Energy Res., **14**: 305-309.

[15] Alam M.S. and Ahammad M.U., 2011. Effects of variable chemical reaction and variable electric conductivity on free convective heat and mass transfer flow along an inclined stretching sheet with variable heat and mass fluxes under the influence of Dufour and Soret effects, Nonlinear Analysis: Modelling and Control, **16**(1): 1–16.

[16] Chen C.H., 2008. Effects of magnetic field and suction/injection on convection heat transfer of non-Newtonian power-law fluids past a power-law stretched sheet with surface heat flux, Int. J.Therm. Sci., **47**(7): 954-961.

[17] Anghel M., Takhar H.S. and Pop I., 2000. Dufour and Soret effects on free convection boundary layer over a vertical surface embedded in a porous medium, Studia Universitatis Babes-Bolyai, Mathematica, **XL**, V: 11–21.

[18] Alam M.S., Rahman M.M. and Samad M.A., 2006. Numerical study of the combined free-forced convection and mass transfer flow past a vertical porous plate in a porous medium with heat generation and thermal diffusion, Nonlinear Anal. Model. Control, **11**(4): 331–343.

[19] Rahman M.M., Billah M.M., Mamun M.A.H., Saidur R. and Hasanuzzaman M., 2010. Reynolds and Prandtl numbers effects on mhd mixed convection in a lid-driven cavity along with joule heating and a centered heat conducting circular block, International journal of mechanical and materials engineering, **5**(2): 163-70.

[20] Ahammad M.U., Rahman M.M. and Rahman M.L., 2012. Effect of inlet and outlet position in a ventilated cavity with a heat generating square block, Engineering e-Transaction **7**(2): 107-115.

[21] Alam M.S. and Rahman M.M., 2012. Thermophoretic particle deposition on unsteady hydromagnetic radiative heat and mass transfer flow along an infinite inclined permeable surface with viscous dissipation and joule heating, Engineering e-Transaction 7(2): 116-126.

[22] Esmaeil Khaje, Kayhani M. H. and Sadi M., 2013. Effect of heat generation on natural convection from an impermeable inclined surface embedded in a porous medium, Journal of Porous Media, **16(5)**: 427-443.

[23] Ahammad, M.U.,Obayedullah Md. And Rahman, M.M.,2013. Analysis of MHD free convection flow along a vertical porous plate embedded in a porous medium with magnetic field and heat generation, *Journal of Engineering e-Transaction (ISSN 1823-6379) Vol |8| Issue|1| Page |10-18|*

[24] Herwig,H.& Gersten,K, Warme and Stafubertr, 20, (1986),P47

[25] Ling, J. X. and Dybbs, A., Forced convection over a flat plate submerged in a porous medium: variable viscosity case, paper 87, Wa/HT-23, (1987), ASME. 9

[26] Lai, F. C. and Kulacki, F.A., The effect of variable viscosity on convective heat and mass transfer along a vertical surface in saturated porous media, Int. J. of Heat and Mass trasfer, Vol. 33 (1991), pp 1028-1031.

[27] Acharya M., Singh L.P. and Dash G.C., 1999. Heat and mass transfer over an accelerating surface with heat source in the presence of blowing, Int. J. Eng. Sci., **37**: 189–211.